

Vol: 20.02

DOI: 10.61164/jzjcha21

Pages: 1-21

COMPUTATIONAL INSIGHTS INTO THE ESTERIFICATION OF LAURIC ACID (C12) WITH $\alpha\textsc{-}BISABOLOL$ OVER CeO $_2$ AS A HETEROGENEOUS CATALYST

PERSPECTIVAS COMPUTACIONAIS SOBRE A ESTERIFICAÇÃO DO ÁCIDO LÁURICO (C12) COM α-BISABOLOL SOBRE CeO₂ COMO CATALISADOR HETEROGÊNEO

Wellington da Conceição Lobato do Nascimento

PhD student in Chemistry – Federal University of Maranhão – UFMA, Brazil Email: wellington.conceicao@discente.ufma.br

Alberto Monteiro dos Santos

Departament of Chemistry – Brandeis University, USA Email: alberto@brandeis.edu

Natanael de Sousa Sousa

PhD in Chemistry – Federal University of Maranhão – UFMA, Brazil Email: 83.natan@gmail.com

Carlos Alberto Lira Júnior

PhD in Biotechnology – Federal University of Maranhão – UFMA, Brazil Email: carlos.lira@ifma.edu.br

Jerônimo Lameira Silva

Institute of Biological Sciences - Federal University of Pará – UFPA, Brazil Email: lameira@ufpa.br

Adeilton Pereira Maciel

Department of Chemistry - Federal University of Rio Grande of Norte – UFRN, Brazil

Email: adeilton.maciel@ufrn.br

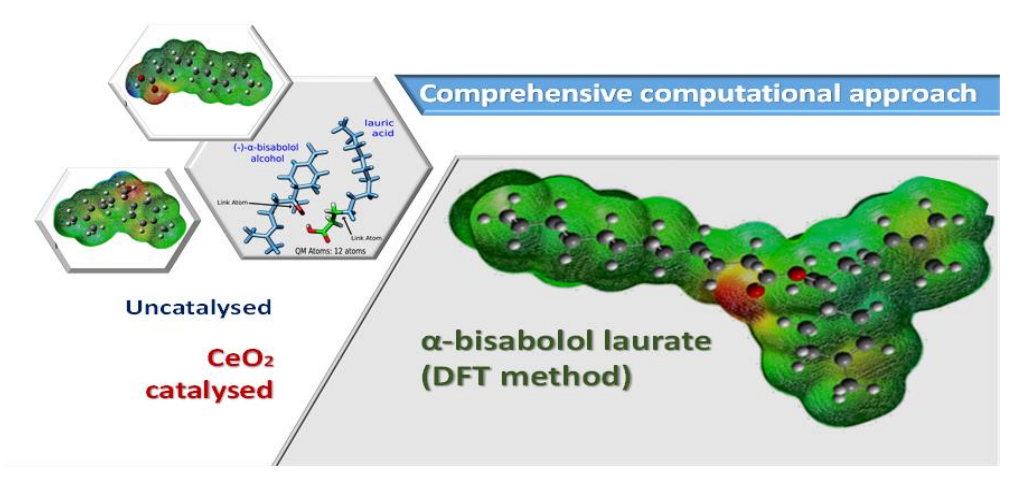


Vol: 20.02

DOI: 10.61164/jzjcha21

Pages: 1-21

Graphical Abstract



Abstract

In this work, we conducted a theoretical investigation of the esterification of lauric acid (C12) with the natural unsaturated alcohol (-)- α -bisabolol, considering both uncatalyzed and CeO₂-catalyzed pathways. Molecular structures were optimized using a combination of semi-empirical methods and Density Functional Theory (DFT), enabling the calculation of key parameters such as dipole moments, electrostatic potential maps, infrared spectra, and frontier molecular orbitals (HOMO and LUMO). For the uncatalyzed reactions, we evaluated thermodynamic descriptors, including enthalpy (Δ H°), Gibbs free energy (Δ G°), and entropy (Δ S°), to gain mechanistic insights. Reaction pathways were further explored through a hybrid QM/MM strategy combined with Molecular Dynamics (MD) simulations. The esterification of lauric acid with (-)- α -bisabolol proceeds via an Sn2-type mechanism. The findings indicate that, in the absence of a catalyst, the reaction is not spontaneous; however, the use of CeO₂ as a heterogeneous catalyst significantly enhances the spontaneity, favoring the formation of (-)- α -bisabolol laurate.

Keywords: Esterification; Heterogeneous catalysis; Lauric acid (C12); α -bisabolol alcohol; Computational chemistry.

Resumo

Neste trabalho, realizamos uma investigação teórica da esterificação do ácido láurico (C12) com o álcool natural insaturado (-)- α -bisabolol, considerando tanto as vias não catalisadas quanto as catalisadas por CeO2. As estruturas moleculares foram otimizadas utilizando uma combinação de métodos semiempíricos e da Teoria do Funcional da Densidade (DFT), permitindo o cálculo de parâmetros-chave, como momentos dipolares, mapas de potencial eletrostático, espectros de infravermelho e orbitais moleculares de fronteira (HOMO e LUMO). Para as reações não catalisadas, avaliamos descritores termodinâmicos, incluindo entalpia (Δ Ho), energia livre de Gibbs (Δ Go) e entropia (Δ So), a fim de obter percepções sobre o mecanismo. As vias reacionais foram ainda exploradas por meio de uma estratégia híbrida QM/MM combinada com simulações de Dinâmica Molecular (MD). A esterificação do ácido láurico com (-)- α -bisabolol ocorre via um mecanismo do tipo SN2. Os resultados indicam que, na ausência de catalisador, a reação não é espontânea; entretanto, o uso de CeO2 como catalisador heterogêneo aumenta significativamente a espontaneidade, favorecendo a formação do laurato de (-)- α -bisabolol.



Vol: 20.02

DOI: 10.61164/jzjcha21

Pages: 1-21

Palavras-chave: Esterificação; Catálise heterogênea; Ácido láurico (C12); Álcool α-bisabolol;

Química computacional.

1. Introduction

The esterification reaction has been extensively investigated due to its fundamental role in the production of higher value-added products from vegetable oils and animal fats [1]. In addition, it is widely applied in various chemical processes to synthesize a broad range of industrially relevant products, including polyethylene terephthalate (PET) [2]. Catalysts are employed to enhance both the reaction rate and yield. Because esterification is a reversible process, an excess of alcohol is typically used to shift the equilibrium toward product formation. Three main categories of catalysts are commonly applied: enzymatic, homogeneous, and heterogeneous [3]. Among them, heterogeneous catalysts offer notable economic advantages due to their reusability, representing a clear benefit over homogeneous systems. In addition, they simplify downstream processing by minimizing the generation of aqueous effluents, allow the use of high-molecular-weight alcohols, and facilitate the separation of glycerol from esters, thereby reducing product purification time [4].

Recently, significant progress has been made in developing heterogeneous catalysts for the production of esters from fatty acids, particularly for industrial applications [5]. In this context, rare earth metals have attracted attention as efficient heterogeneous catalysts. Among them, CeO₂ stands out due to its remarkable oxygen storage capacity, high thermal stability, and notable optical, electrical, and diffusional properties [6], which underpin its wide range of technological applications.

Vegetable oils are regarded as a promising feedstock for the production of diverse industrial products, owing to their renewable availability, abundance, and environmental benefits. Esterification has been widely employed to obtain esters from various vegetable oils, such as soybean, sunflower, babassu, castor, palm kernel, and palm, among others [7]. In particular, the oil extracted from babassu



Vol: 20.02

DOI: 10.61164/jzjcha21

Pages: 1-21

coconut (*Attalea speciosa* Mart. ex Spreng.) is noteworthy for its high lauric acid (C12:0) content, and has recently been applied in esterification processes [8,9].

The babassu coconut is an ellipsoid-shaped fruit that grows on palm trees widely distributed across the North and Northeast regions of Brazil. Its primary product is the oil extracted from the kernels, which is highly valued in the chemical, cosmetic, biofuel, and food industries [10]. Babassu oil is composed predominantly of saturated fatty acids, with lauric acid as the major component, followed by myristic, palmitic, stearic, oleic, linoleic, capric, and caprylic acids [9]. One strategy for increasing the value of babassu coconut components is to transform them into high-value commercial products. Babassu oil can be transesterified with various alcohols, including α -bisabolol, a chain-long alcohol gaining attention in the transformation industry [11].

The α -bisabolol is a natural monocyclic sesquiterpenoid that has been formally identified as (-)- α -bisabolol and is also known as levomenol. Its official IUPAC name is (2S)-6-methyl-2-[(1S)-4-methylcyclohex-3-en-1-yl)]hept-5-en-2-ol. α -bisabolol has a molecular weight of 222.37 g/mol, low density (0.922–0.931) g/cm³, XLogP3-AA (3.8) and logP (5.070). This alcohol exhibits anti-inflammatory, antiseptic, bactericidal, antimycotic, and healing properties. Although α -bisabolol is widely used in the industry, little is known about the molecular-level esterification reactions [12].

Understanding the esterification reaction mechanism can be useful for optimizing process parameters, enhancing yield, and ensuring product consistency, especially in the context of biodiesel production and other industrial applications. Computational studies, particularly employing Density Functional Theory (DFT), have significantly contributed to this understanding. For example, direct oxidative esterification employing Ni/Au-based catalysts for the synthesis of methyl methacrylate (MMA) from methacrolein and methanol was investigated with the support of DFT calculations and experimental data [13]. In another study, heterogeneous catalysts containing Cu were applied in the synthesis of chiral allylic esters, achieving a 90% yield and an enantiomeric excess of 77%. In this case, the



Vol: 20.02

DOI: 10.61164/jzjcha21

Pages: 1-21

formation mechanism of the esters was elucidated through density functional theory (DFT) calculations [14]. These findings emphasize the role of computational analysis in optimizing esterification processes.

In this study, we employed a comprehensive computational approach to investigate the esterification of lauric acid with α -bisabolol, both in the presence and absence of the heterogeneous catalyst CeO₂, with an emphasis on the effects of steric hindrance. The aim was to optimize the reaction conditions involving lauric acid (C12) and α -bisabolol, addressing the gap in the theoretical analysis of the esterification of vegetable oils with long-chain alcohols in heterogeneous catalytic systems. The results provide new insights into the mechanisms underlying this type of reaction and contribute to the development of more efficient and environmentally sustainable industrial processes.

2. Computational Methodology

2.1 System preparation

Initially, geometry optimizations were performed using Gaussian 09 and PM6 (Parametric Method 6) level [15]. The calculation procedure consists of optimizing the structures of the molecules to obtain energy parameters such as: dipole moment vectors, electrostatic potential surface map (MEP), infrared spectroscopy (IR), the energy of HOMO and LUMO molecular orbitals.

The structure of the CeO₂ catalyst had its geometry fully optimized as energy minima using the HF-3c method (the structures of the reactants and products were optimized in the uncatalysed reactions) [16].

Following the optimization of the catalyst, the reactant-catalyst system was assembled (for the esterification reactions) to obtain the free energy of the reactions using the DFT method (M062X/6-31+G (d,p)) [17].

2.2 The potential energy surface (PES)



Vol: 20.02

DOI: 10.61164/jzjcha21

Pages: 1-21

We examined the catalysed and uncatalysed esterification reactions of C12 lauric acid with (-)-α-bisabolol alcohol using various potential energy surfaces (PES), employing the pDynamo library for molecular modeling and ORCA for quantum mechanical (QM) calculations [18, 19]. Despite its limitations in evaluating free energy surfaces in enzymatic reactions due the limited sampling, PES allows the inclusion QM/MM potential in the simulations due its low computational cost. In the QM/MM approach a small part of the system involved in the mechanism is described by quantum mechanics, while MM force fields represent the contour region. The 2D potential energy surfaces (PESs) for esterification reactions were obtained for both catalysed and uncatalysed mechanisms. The QM region was described using the M06-2X/6-31+G(d,p) potential, and the atomic coordinates of reacting atoms were restrained by a harmonic umbrella potential of 50 kcal·mol⁻¹ Å². Additionally, we constructed 2D PESs using PM6, HF-3c, and B3LYP methods to compare with M06-2X/6-31+G(d,p) results, with transition states identified as saddle points. For the hybrid QM/MM calculations, the atoms of the lauric acid and alcohol (-)-α-bisabolol moieties were selected to be treated by QM, using a semi-empirical PM6 [15] and M06-2X/6-31+G(d,p) potential [17].

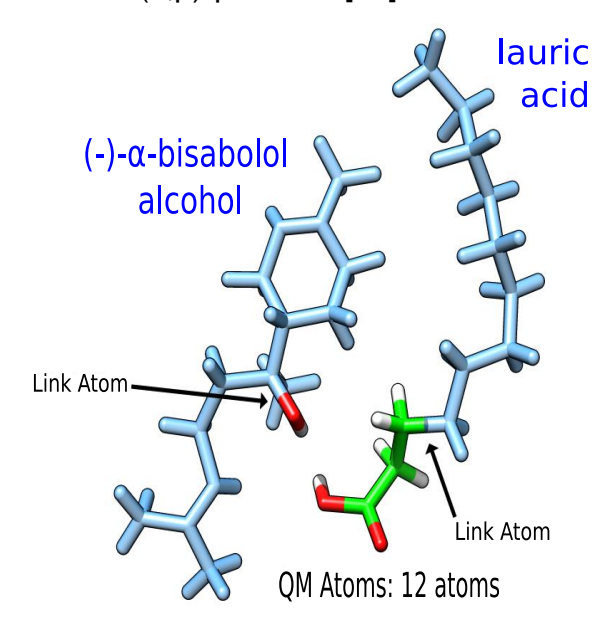


Figure 1. Quantum Region for the non-catalysed reaction.



Vol: 20.02

DOI: 10.61164/jzjcha21

Pages: 1-21

The other atoms of the system were described using the CHARMM36 [20] force field. The number of QM atoms resulted then to be 79 while the final system contains 12 atoms, respectively. To investigate the mechanism, a 2D-PES was initially created using the R1-R2 combination that corresponds to the addition/elimination stages of lauric acid and (-)-α-bisabolol alcohol, as well as the R2-R3 distance, which corresponds to the proton transfer to the water molecule (Figure 1).

3. Results and Discussion

3.1 Dipole moments, electrostatic surface potential, homo and lumo and spectra infrared

The dipole moment magnitudes were calculated for the optimized molecular structures. Expressed in Debye (D), the dipole moment represents the product of the partial charges and the distance separating the most electronegative regions of the molecule. The dipole moments of the studied molecules were obtained using the PM6 method [15] (Table 1).

Table 1. Molecular dipole moment for the structures.

Chemical compounds	Dipole moment (Debyes)
Lauric acid	1.15
(-)-α-bisabolol	1.34
(-)-α-bisabolol laurate	1.72

Table 1 shows that, among the reactants, lauric acid exhibited a dipole moment of 1.15 D, while (–)-α-bisabolol presented 1.34 D. The reaction product, (–)-α-bisabolol laurate, showed a value of 1.72 D, indicating higher molecular polarity. It is well established that the affinity of a molecule for polar environments increases with its dipole moment, which consequently tends to raise its melting and boiling points.



Vol: 20.02

DOI: 10.61164/jzjcha21

Pages: 1-21

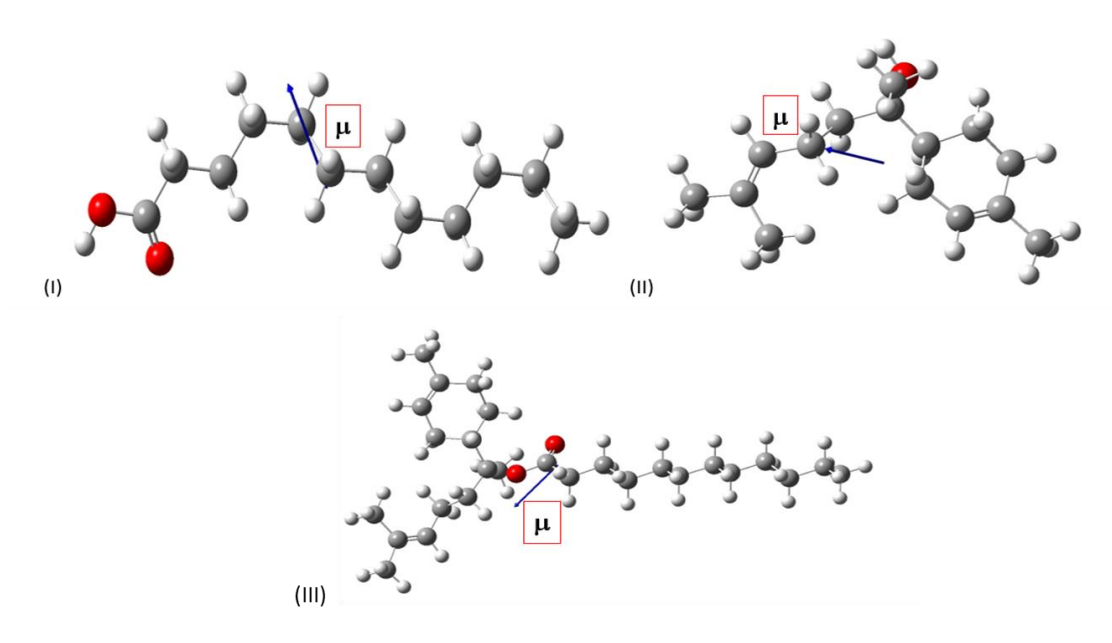
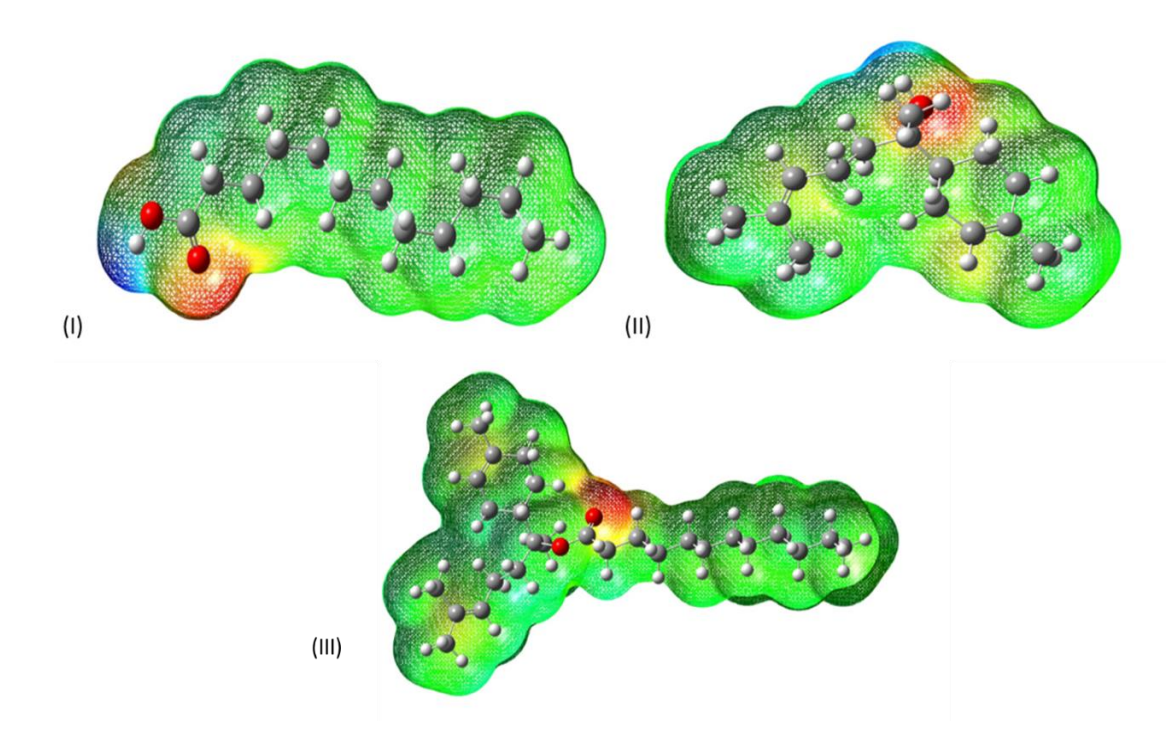


Figure 2. Optimized structures and representation of the vectorial resultant of the electronegative dipole moment of (I) lauric acid (C12), (II) (-)- α -bisabolol and (III) (-)- α -bisabolol laurate.

Figure 2 illustrates that the dipole moment vector (μ) originates in regions of lower electronic density and points toward regions of higher electronic density, indicating both an increase in polarity and in vector magnitude along this direction.





Vol: 20.02

DOI: 10.61164/jzjcha21

Pages: 1-21

Figure 3. Molecular electrostatic potential (MEP) for: (I) lauric acid (C12), (II) (-)- α -bisabolol and (III) (-)- α -bisabolol laurate using the DFT method.

The Molecular Electrostatic Potential (MEP) map, first introduced by Reed et al. in 1985 [21], offers a visual approach to assessing the relative polarity of molecules. By identifying nucleophilic and electrophilic sites, and when combined with dipole moment data, MEP maps enable predictions of the types of intermolecular interactions likely to occur [22]. Figure 3 presents the ESP maps of the reactants and products involved in the non-catalyzed esterification reactions. Two distinct regions are observed: (i) nucleophilic domains, mainly localized around oxygen atoms, and (ii) electrophilic domains, primarily associated with hydrogen and carbon atoms.

The active site of the uncatalyzed esterification reaction was identified at the carbonyl group of lauric acid and the hydroxyl group of the alcohol (-)- α -bisabolol. Specifically, in the uncatalyzed pathway, the carbonyl region of the C12 lauric acid consistent with the dipole moment results and the hydroxyl region of (-)- α -bisabolol act as the reactive centers.

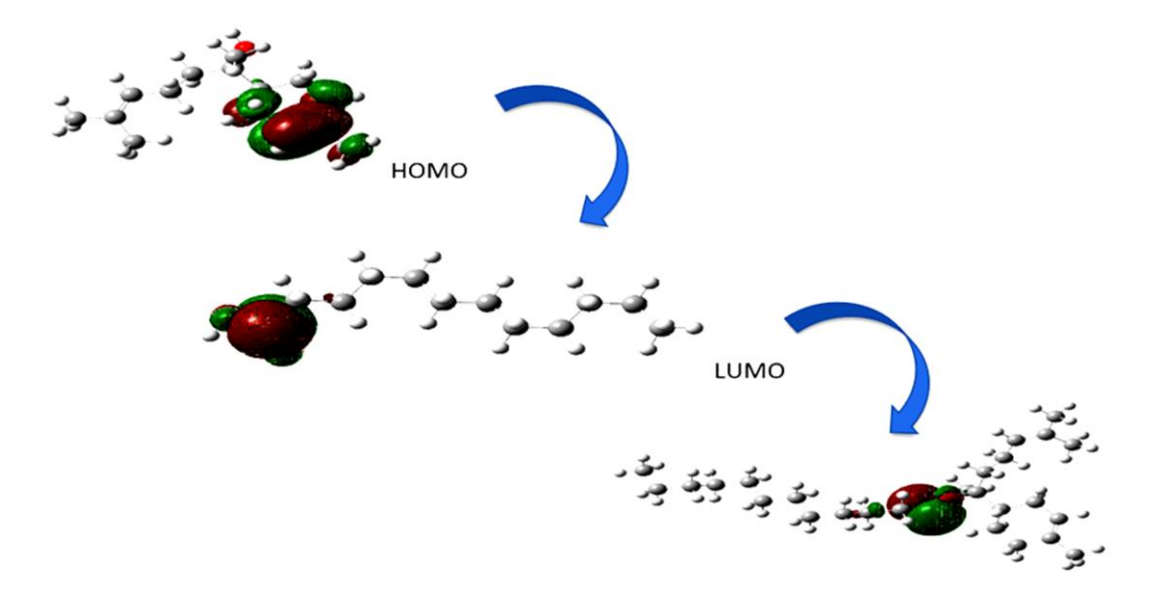


Figure 4. Proposed nucleophilic attack of the HOMO orbital of $(-)-\alpha$ -bisabolol on the LUMO orbital of lauric acid.



Vol: 20.02

DOI: 10.61164/jzjcha21

Pages: 1-21

Figure 4 presents the HOMO and LUMO molecular orbitals, obtained using the PM6 method, for both the reactants and products of the non-catalyzed esterification reactions. In chemical reactions, effective interaction occurs through the overlap of the HOMO of the negative species (the nucleophile) with the LUMO of the positive species (the substrate or electrophile) [23]. In this case, the HOMO of (-)- α -bisabolol functions as the nucleophile, attacking the LUMO of lauric acid.

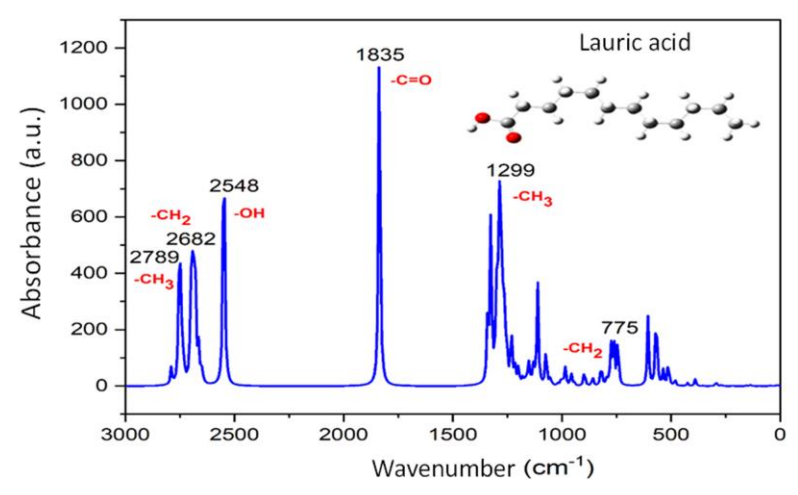


Figure 5. The infrared spectrum for lauric acid obtained through the PM6 computational method.

The infrared spectra of the molecules were calculated using the PM6 method. In lauric acid (Figure 5), the vibrational modes correspond to CH3 and CH2 stretching. A key spectral feature is a strong band attributed to the C=O bond at 1835 cm⁻¹, along with a medium-intensity band corresponding to OH stretching at 2548 cm⁻¹. Angular deformations of CH3 and CH2 appear at 1299 cm⁻¹ and 775 cm⁻¹, respectively. Some of the calculated frequencies deviate from experimental values; for example, the C=O vibration is typically observed around 1700 cm⁻¹ [24].

Figure 6 shows the infrared spectrum of (–)-α-bisabolol, with absorption bands in the 2792–2775 cm⁻¹ region corresponding to CH₃ and CH₂ stretching. As a tertiary and chiral alcohol, a strong band at 2699 cm⁻¹ is assigned to the C-chiral CH₃ stretch. The spectrum presents two characteristic regions: a medium-intensity band attributed to OH stretching at 2543 cm⁻¹ and a C=C deformation band at 1812 cm⁻¹, indicating the presence of two unsaturations in the molecule. The angular



Vol: 20.02

DOI: 10.61164/jzjcha21

Pages: 1-21

deformation of the chiral center appears at 1361 cm⁻¹, while additional deformations are observed for CH₃ at 1257 cm⁻¹ and =CH at 807 cm⁻¹, the latter corresponding to a low-intensity band [25].

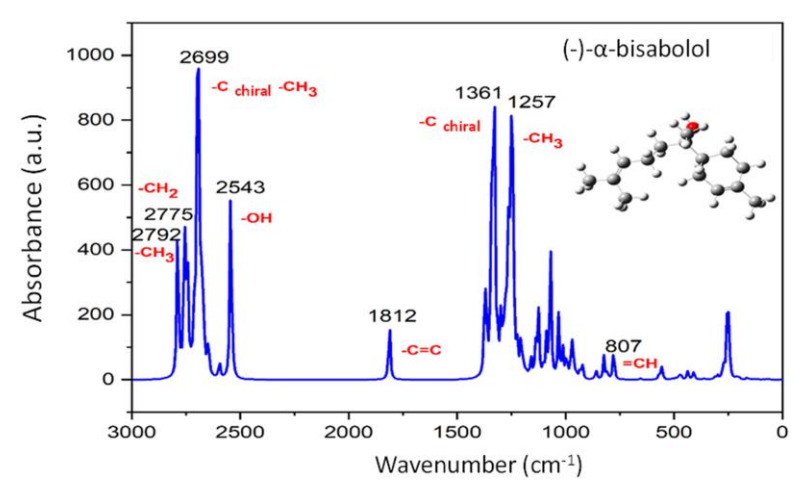


Figure 6. Infrared spectrum obtained by the PM6 computational method for the alcohol (-)- α -bisabolol.

The Figure 7 shows the spectrum of the (-)-α-bisabolol laurate molecule. The region between 2789 and 2692 cm⁻¹ corresponds to CH₃ and CH₂ stretching. The spectrum shows two overlapping peaks with intensities of 1803 and 1813 cm⁻¹, corresponding to C=O and C=C, respectively. The (-)-bisabolol laurate molecule consists of a chiral carbon, which has been attributed to the angular deformation of C-chiral at 843 cm⁻¹ and a band of low intensity attributed to C-O at 687 cm⁻¹.

In view of its attack on the lauric acid C12 to form laurate (-)- α -bisabolol, the region at 2548 cm⁻¹ related to the OH stretching of the alcohol (-)- α -bisabolol is in fact the most important for understanding the uncatalysed esterification reaction.



Vol: 20.02

DOI: 10.61164/jzjcha21

Pages: 1-21

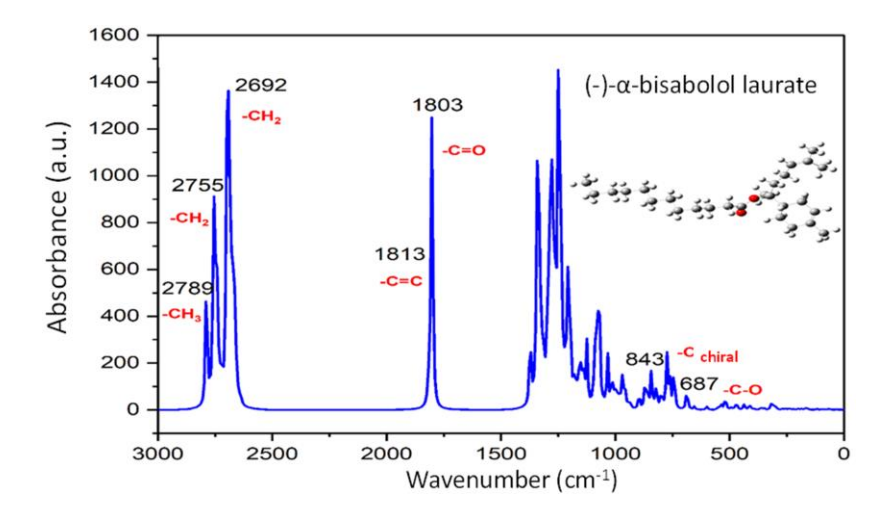


Figure 7. Infrared spectrum obtained by the PM6 computational method for $(-)-\alpha$ -bisabolol laurate.

3.2 Uncatalysed Esterification Reaction of Lauric Acid with (-)-α-Bisabolol

The uncatalyzed and catalyzed esterification reactions were evaluated using the PM6 method and DFT calculations at the B3LYP/6-31+G level to assess their spontaneity. To elucidate the mechanism of the uncatalyzed esterification of lauric acid with (-)- α -bisabolol, potential energy surface and frequency calculations were carried out with the HF-3c and PM6 methods.

From these analyses, thermodynamic and kinetic parameters were obtained, including ΔH , ΔS , ΔG , $\Delta G\ddagger$, and the rate constant. All calculations were performed under STP conditions, as described in the Methods section. According to the computational results (Table 2 and Figure 8), the uncatalyzed esterification of lauric acid with (–)- α -bisabolol is exothermic ($\Delta H^0 = -0.29 \text{ kcal·mol}^{-1}$). However, the Gibbs free energy ($\Delta G^0 = 24.7 \text{ kcal·mol}^{-1}$) reveals that the process is not thermodynamically favorable, indicating that the reaction is non-spontaneous.



Vol: 20.02

DOI: 10.61164/jzjcha21

Pages: 1-21

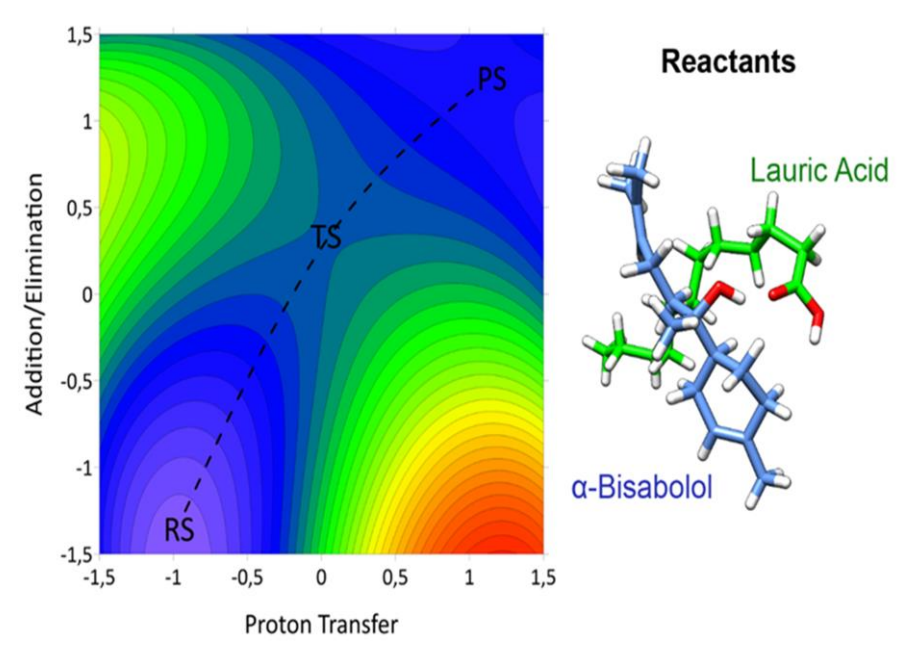


Figure 8. SEP2D. Each line corresponds to 5 kcal.

Table 2. Thermodynamic and kinetic parameters for the uncatalysed esterification reaction.

Lauric acid + (-)- α -Bisabolol \rightarrow (-)- α -Bisabolol laurate + H₂O $\Delta H^0 = -0.29 \text{ kcal.mol}^{-1}$ $\Delta S^0 = -0.08 \text{ kcal.K.mol}^{-1}$ $\Delta G^0 = 24.70 \text{ kcal.mol}^{-1}$ $\Delta G^{\ddagger} = 42.80 \text{ kcal.mol}^{-1}$ $k = 4.856 \times 10^{-6} \text{ s}^{-1}$

 ΔH^o - Enthalpy of reaction; ΔS^o - Entropy of reaction; ΔG^o - Gibbs free energy.

ΔG[‡] - Activation energy; k - Reaction rate constant.

The optimized structures of lauric acid and (–)- α -bisabolol, illustrating the esterification reaction pathway, are shown in Figure 8. During the formation of (–)- α -bisabolol laurate, a water molecule is released through the interaction between the hydroxyl group of the alcohol and the carbonyl group of lauric acid. The reaction was modeled using the DFT method (B3LYP) with the 6-31+G basis set. The transition state (TS) was confirmed by the presence of a single imaginary frequency at -1242.46 cm⁻¹, corresponding to a first-order saddle point (Figure 9).



Vol: 20.02

DOI: 10.61164/jzjcha21

Pages: 1-21

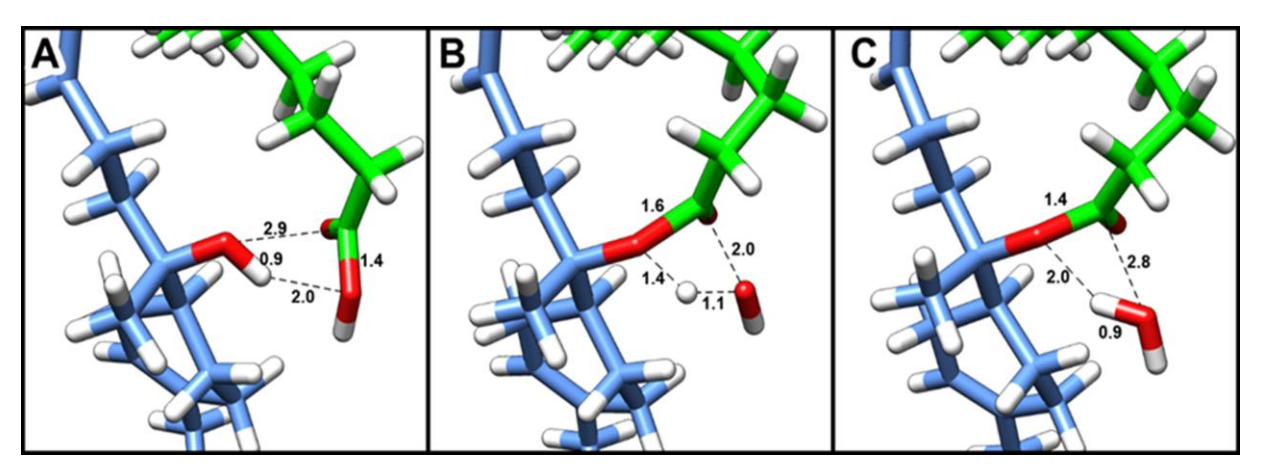


Figure 9. Transition geometries of the uncatalysed esterification reaction.

3.4 Esterification Reaction of Lauric Acid with (-)- α -Bisabolol Catalysed by CeO_2

After demonstrating that the uncatalyzed esterification reactions are non-spontaneous, we performed theoretical QM/MM MD calculations with a heterogeneous CeO₂ catalyst to assess the spontaneity of the reaction between lauric acid and (–)-α-bisabolol. The initial calculations followed the same DFT methodology (B3LYP) used for the uncatalyzed reactions. However, due to the high computational cost, the HF-3c method was employed to obtain the initial optimized structures of the catalyst–reactant complexes.

Figure 10 presents the structures of the catalyst and reactants obtained from QM/MM MD calculations. To achieve more accurate energies, the DFT method (M06-2X/6-31+G(d,p)) was employed, although no significant differences in energy magnitudes were observed compared to the B3LYP method. The calculations of the esterification reaction with the CeO₂ catalyst indicate minimal energy differences between the transition state (TS) and the product state (PS), suggesting that the reactant state (RS) converges directly to the PS, in contrast to the TS identified in vacuum conditions.

Mucelini et al. [26] investigated the adsorption of zirconium atoms on cerium oxide surfaces: Zn/CeO₂ (111). The study examined the nature and magnitude of



Vol: 20.02

DOI: 10.61164/jzjcha21

Pages: 1-21

the interactions between Zr and CeO₂ (111) atoms in terms of the electronic, geometric, and energetic properties of the materials. The surface of CeO₂ (111) exhibited layers of a single type of atom in the ratio of one Ce layer to two O layers, which could be stacked as repeats of O-Ce-O or O-O-Ce, with each atom representing a layer. Only the O-Ce-O termination was studied because it is more stable than the O-O-Ce termination.

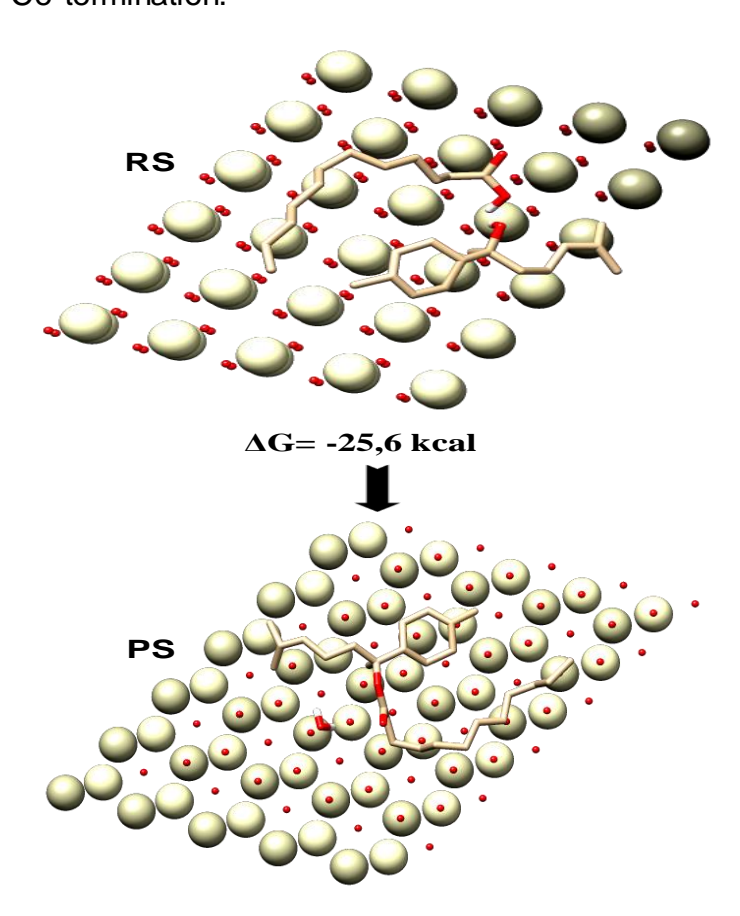


Figure 10. Optimized geometries of the interaction between lauric acid molecules and $(-)-\alpha$ -bisabolol alcohol catalysed with CeO₂ obtained by the DFT computational method (M062X 6-31+G(d,p)).

Esterification calculations of lauric acid and the alcohol (-)- α -bisabolol with the CeO₂ catalyst showed that the energy obtained was ΔG = -25.62 Kcal for the conversion of (-)- α -bisabolol to the product laurate, indicating that this reaction occurs spontaneously.



Vol: 20.02

DOI: 10.61164/jzjcha21

Pages: 1-21

4. Conclusions

In both catalyzed and uncatalyzed reactions, factors such as steric hindrance between the nucleophile and the electrophile have a significant impact on the progress of the esterification reaction. Computational studies revealed that a concerted SN2-type mechanism directly converting reactants into products during the transition state governs the interaction between the reactants in both reaction types. Lauric acid (C12) does not react spontaneously with (–)- α -bisabolol, as demonstrated by DFT (B3LYP) simulations. In the CeO₂-catalyzed process, DFT calculations (M06-2X/6-31+G(d,p)) showed that the reaction of lauric acid with (–)- α -bisabolol becomes thermodynamically favorable. Considering the limited theoretical studies on the heterogeneous catalytic esterification of vegetable oils with long-chain alcohols, this work provides important contributions to the scientific community and opens new avenues for future research.

Data Availability Statement

The data that support the findings of this study are available from the corresponding author upon reasonable request.

Conflicts of Interest

The authors declare no conflicts of interest.

Funding

This study was supported by FAPEMA - Foundation for Research and Scientific and Technological Development of Maranhão, project number BM-01113/20.

Acknowledgments

This work has been supported by the following Brazilian research agencies: National Council for Scientific and Technological Development (CNPq),



Vol: 20.02

DOI: 10.61164/jzjcha21

Pages: 1-21

304205/2018-4, National Council for the Improvement of Higher Education (CAPES), Finance Code 001, Maranhão Research and Scientific and Technological Development Support Foundation (FAPEMA). The first author received fellowships from FAPEMA (BM-01113/20).

References

[1] Bhatia SK, Bhatia RK, Jeon J, Pugazhendhi A, Awasthi MK, Kumar D, Kumar G, Yoon J, Yang Y (2021) An overview on advancements in biobased transesterification methods for biodiesel production: Oil resources, extraction, biocatalysts, and process intensification technologies, Fuel. 285:119117. https://doi.org/10.1016/j.fuel.2020.119117.

- [2] Derr KM, Lopez CV, Maladeniya CP, Tennyson AG, Smith RC (2023) Transesterification-vulcanization route to durable composites from post-consumer poly (ethylene terephthalate), terpenoids, and industrial waste sulfur, J. Polym. Sci. 61:3075-3086. https://doi.org/10.1002/pol.20230503.
- [3] Baskar G, Aiswarya R (2016) Trends in catalytic production of biodiesel from various feedstocks. Renew. and Sustain. Energy Rev. 57:496-504. https://doi.org/10.1016/j.rser.2015.12.101.
- [4] Suppes GJ, Bockwinkel K, Lucas S, Botts JB, Mason MH, Heppert JA (2001) Calcium Carbonate Catalyzed of Fat and Oils, J Am Oil Chem Soc. 78:139-146. https://doi.org/10.1007/s11746-001-0234-y.
- [5] Appaturi JN, Andas J, Ma YK, Phoon BL, Batagarawa SM, Khoerunnisa F, Hussin MZ, Ng EP (2022) Recent advances in heterogeneous catalysts for the synthesis of alkyl levulinate biofuel additives from renewable levulinic acid: A comprehensive review, Fuel 323:124362. https://doi.org/10.1016/j.fuel.2022.124362.



Vol: 20.02

DOI: 10.61164/jzjcha21

Pages: 1-21

[6] Trovarelli A., Catalysis by ceria and Related Materials. 2. ed. Imperial College Press, London. 2002. https://doi.org/10.1142/p249.

[7] Elgharbawy AS, Sadik WA, Sadek OM, Kasaby MA (2021) A review on biodiesel feedstocks and production technologies, J. Chil. Chem. Soc. 66:5098–5106. https://dx.doi.org/10.4067/S0717-97072021000105098.

[8] Matsue M, Mori Y, Nagase S, Sugiyama Y, Hirano R, Ogai K, Ogura K, Kurihara S, Okamoto S. (2019) Measuring the Antimicrobial Activity of Lauric Acid against Various Bacteria in Human Gut Microbiota Using a New Method, Cell Transplant. 28:1258–1268. https://dx.doi.org/10.1177/0963689719881366.

[9] Alexandre JYNH, Cavalcante FTT, Freitas LM, Castro AP, Borges PT, Sousa Junior PG, Filho MNR, Lopes ASS, Fonseca AM, Lomonaco D, Rios MAS, Santos JCS (2022) A Theoretical and Experimental Study for Enzymatic Biodiesel Production from Babassu Oil (Orbignya sp.) Using Eversa Lipase, Catalysts 12:1322. https://doi.org/10.3390/catal12111322.

[10] Rangel NVP, Silva LP, Pinheiro VS, Figueredo IM, Campos OS, Costa SN, Luna FMT, Cavalcante Jr. CL, Marinho ES, Lima-Neto P, Maria Rios MA (2021) Effect of additives on the oxidative stability and corrosivity of biodiesel samples derived from babassu oil and residual frying oil: An experimental and theoretical assessment, Fuel. 291:119939. https://doi.org/10.1016/j.fuel.2020.119939.

[11] Maciel AP (2016) Babassu biofuels: technical essay on opportunities for producing biofuels from babassu coconut. *EDUFMA*, São Luís-MA, Brazil.

[12] Souza ERL, Gomes NML, J. H. A. (2021) Propriedades farmacológicas do Sesquiterpeno α-Bisabolol: uma breve revisão. Arch Health Invest., 10:1–6. https://doi.org/10.21270/archi.v10i1.3183.

[13] Tan H, Lou B, Shen A & Ning C. (2023) Experimental and theoretical research on one-step oxidative esterification of methyl acrolein with methanol. Ind. Eng. Chem. Res., 62:21609-21618. https://doi.org/10.1021/acs.iecr.3c03136.



Vol: 20.02

DOI: 10.61164/jzjcha21

Pages: 1-21

[14] Majidian S, Rashid HI, Naghdi Y, Irani M, & Samadi S. (2025) Copper-Catalyzed Simultaneous Dehydrogenation and Enantioselective Allylic Oxidation of Alkanes Using Chiral Heterogeneous Ligands to Produce Allylic Esters and Theoretical Investigation of the Mechanism. Appl. Organomet. Chem., 39:e7857. https://doi.org/10.1002/aoc.7857.

[15] Stewart JJP (2009) Application of the PM6 method to modeling the solid state, J. Mol. Model., 15:765–805. https://doi.org/10.1007/s00894-008-0299-7.

[16] Praveen PA, Saravanapriya D, Bhat SV, Arulkannan K, Kanagasekaran T (2024) Comprehensive analysis of DFT-3C methods with B3LYP and experimental data to model optoelectronic properties of tetracene, Mat. Sci. Semicond. Process., 158:108159. https://doi.org/10.1016/j.mssp.2024.108159.

[17] Zhao Y, Truhlar DG (2008) The M06 suite of density functionals for main group thermochemistry, thermochemical kinetics, noncovalent interactions, excited states, and transition elements: two new functionals and systematic testing of four M06-class functionals and 12 other functionals, Theor. Chem. Account. 120:215–241. https://doi.org/10.1007/s00214-007-0310-x.

[18] Field MJ (2008) *The pDynamo Program for Molecular Simulations using Hybrid Quantum Chemical and Molecular Mechanical Potentials, J. Chem. Theory Comput.*, 4:1151–1161. https://doi.org/10.1021/ct800092p.

[19] Neese F, Wennmohs F, Becker U, Riplinger C (2020) The ORCA quantum chemistry program package, *J. Chem. Phys.*, 152:224108. https://doi.org/10.1063/5.0004608.

[20] Zhu X, Lopes PEM, MacKerell Jr AD (2013) Recent developments and applications of the CHARMM force fields, WIREs Comput Mol Sci., 3:386–408. https://doi.org/10.1002/wcms.74.

[21] Reed AE, Weinhold F (1985) Natural Population Analysis. J Chem Phys., 83:735–746. https://doi.org/10.1063/1.449486.



Vol: 20.02

DOI: 10.61164/jzjcha21

Pages: 1-21

[22] Politzer P, Murray J (2002) The fundamental nature and role of the electrostatic potential in atoms and molecules, Theor Chem Acc., 108:134–142. https://doi.org/10.1007/s00214-002-0363-9.

[23] Fleming (1976) Frontier Orbitals and Organic Chemical Reactions. John Wiley & Sons, New York.

[24] Sinclair RG, McKay AF, Jones RN (1952) The infrared absorption spectra of saturated fatty acids and esters, J. Am. Chem. Soc., 74:6070–6075. https://doi.org/10.1021/ja01130a033.

[25] Oliveira FS, Freitas TS, Cruz RP, Costa MS, Pereira RLS, Quintans-Júnior LJ, Andrade TA, Menezes PP, Sousa BMH, Nunes PS, Serafini MR, Menezes IRA, Araújo AAS, Coutinho HDM (2017) Evaluation of the antibacterial and modulatory potential of a-bisabolol, b-cyclodextrin and a-bisabolol/b-cyclodextrin complex, Biomed Pharmacother 93:87–94. https://doi.org/10.1016/j.biopha.2017.06.020.

[26] Mucelini J, Costa-Amaral R, Seminovski Y, Silva JLF (2018) Ab initio investigation of the formation of ZrO₂-like structures upon the adsorption of Zrn on the CeO₂ (111) surface, J. Chem. Phys., 149:164701. https://doi.org/10.1063/1.5063732.